

Administration of the glutamate-modulating drug, riluzole, after stress prevents its delayed effects on the amygdala in male rats

Siddhartha Datta^{a,†}, Zubin Rashid^{a,†}, Saptarnab Naskar^b and Sumantra Chattarji^{a,*}

^aNational Centre for Biological Sciences, Tata Institute of Fundamental Research, Bangalore 560065, India

^bDepartment of Psychiatry and Behavioral Sciences, Northwestern University, Feinberg School of Medicine, Chicago, IL 60611, USA

*To whom correspondence should be addressed: Email: shona@ncbs.res.in

[†]S.D. and Z.R. contributed equally to this work.

Edited By: Eric Klann

Abstract

Extracellular glutamate levels are elevated across brain regions immediately after stress. Despite sharing common features in their genesis, the patterns of stress-induced plasticity that eventually take shape are strikingly different between these brain areas. While stress causes structural and functional deficits in the hippocampus, it has the opposite effect on the amygdala. Riluzole, an FDA-approved drug known to modulate glutamate release and facilitate glutamate clearance, prevents stress-induced deficits in the hippocampus. But whether the same drug is also effective in countering the opposite effects of stress in the amygdala remains unexplored. We addressed this question by using a rat model wherein even a single 2-h acute immobilization stress causes a delayed expression of anxiety-like behavior, 10 days later, alongside stronger excitatory synaptic connectivity in the basolateral amygdala (BLA). This temporal profile—several days separating the acute stressor and its delayed impact—allowed us to test if these effects can be prevented by administering riluzole in drinking water *after* acute stress. Poststress riluzole not only prevented the delayed increase in anxiety-like behavior on the elevated plus maze but also blocked the increase in spine density on BLA neurons 10 days later. Further, stress-induced increase in the frequency of miniature excitatory postsynaptic currents recorded in BLA slices, 10 days later, was also blocked by the same poststress riluzole administration. Together, these findings underscore the importance of therapeutic strategies, aimed at glutamate uptake and modulation, in correcting the delayed behavioral, physiological, and morphological effects of stress on the amygdala.

Keywords: acute immobilization stress, riluzole, spine plasticity, excitatory synapses, anxiety

Significance Statement

Stress disorders are characterized by impaired cognitive function alongside enhanced emotionality. Consistent with this, the same stress elicits contrasting effects in the rodent hippocampus versus amygdala. This poses a therapeutic challenge—the same pharmacological intervention against stress has to counter these opposite effects. Yet, the immediate consequence of stress—enhanced extracellular glutamate—is similar across these two areas. To target this common feature, we treated rats with riluzole, a drug that prevents stress-induced glutamate surge. Although the drug was administered after the end of stress, it blocked its delayed impact on amygdalar structure and function. Since riluzole also enhances glutamate uptake through glial transporters and is approved for human use, these results highlight the importance of therapeutic strategies focused on neuron–astrocyte interactions.

Introduction

The amygdala, a brain structure that is necessary for the encoding of emotionally salient memories, is susceptible to stressful experiences (1, 2). Accumulating evidence from animal models has showed that stress leads to significant changes in the structure and function of amygdalar neurons, including growth of dendrites and spines, and increased transmission and plasticity at excitatory synapses (3, 4). Stress also enhances conditioned fear and anxiety-like behavior (1, 5–8). Together, these findings on

stress-induced plasticity in the amygdala offer insights into the exaggerated affective symptoms seen in stress-related neuropsychiatric disorders (3, 4, 9–12). Increase in extracellular glutamate levels and glutamatergic transmission in the amygdala is one of the immediate consequences of stress (13, 14). Hence, in this study, we test the hypothesis that pharmacological attenuation of poststress elevation in glutamate levels and glutamatergic transmission in the amygdala should prevent the delayed cellular and behavioral effects of stress.

Competing Interest: The authors declare no competing interest.

Received: March 8, 2023. **Revised:** May 5, 2023. **Accepted:** May 15, 2023

© The Author(s) 2023. Published by Oxford University Press on behalf of National Academy of Sciences. This is an Open Access article distributed under the terms of the Creative Commons Attribution-NonCommercial-NoDerivs licence (<https://creativecommons.org/licenses/by-nc-nd/4.0/>), which permits non-commercial reproduction and distribution of the work, in any medium, provided the original work is not altered or transformed in any way, and that the work is properly cited. For commercial re-use, please contact journals.permissions@oup.com

Further, instead of pharmacological interventions before or during stress, a clinically realistic paradigm would entail administering drugs *after* the stressful experience. It is in this context that a rodent model of acute immobilization stress offers an important advantage due to the unique temporal profile of changes it triggers in the amygdala (3, 15–17). Specifically, a single 2-h episode of immobilization stress leads to delayed morphological and physiological strengthening of synaptic connectivity in the basolateral amygdala (BLA), along with enhanced anxiety-like behavior, 10 days later (15–17). Thus, this rat model presents a window for poststress intervention to prevent the immediate stress-induced increase of glutamate and then test if the delayed neuronal and behavioral effects, 10 days later, can be blocked.

Riluzole, a compound that enhances glutamate uptake, modulates glutamate release, inhibits postsynaptic glutamate receptors (18–23), and offers several advantages as a poststress pharmacological intervention. First, this drug is approved for use in patients of amyotrophic lateral sclerosis (ALS) (24–27) because it counteracts glutamate excitotoxicity (28) by enhancing glutamate uptake mediated by the astrocytic transporters, GLT-1 and GLAST (19, 20), as well as attenuating presynaptic glutamate release (22). Further, riluzole is soluble in drinking water and, hence, bypasses the need for stressful interventions such as intraperitoneal injections or oral gavage in rodents (29, 30). Interestingly, riluzole administered before or during chronic stress has been shown to block its effects in the hippocampus and prefrontal cortex (PFC) (31–34). However, nothing is known about the efficacy of poststress riluzole administration in preventing the delayed impact of acute stress in the amygdala. Hence, in the present study, we examined if administration of riluzole in drinking water after stress is effective in blocking the delayed behavioral, structural, and physiological effects in the amygdala.

Results

Oral administration of riluzole after acute stress prevents its delayed anxiogenic effects

A single episode of 2-h immobilization stress has been reported to cause a delayed anxiogenic effect (16, 29, 30, 35). We, therefore, wanted to first reproduce this result before examining the efficacy of any poststress pharmacological intervention (Fig. 1A). In the elevated plus maze (EPM) task, we observed a significant reduction in the percentage of time spent in the open arm (Fig. 1B: Control: $61.3 \pm 2.9\%$; Stress: $37.1 \pm 5.3\%$, $N = 16$ rats per group) 10 days after acute immobilization stress. This was also paralleled by a decrease in the percentage of entries into the open arm (Fig. 1C: Control: $68.0 \pm 1.9\%$; Stress: $41.6 \pm 5.0\%$). Together, these changes were reflected as a significant increase in the anxiety index (see Materials and methods) in the stressed rats (Fig. 1D: Control: 0.35 ± 0.02 ; Stress: 0.61 ± 0.05). Thus, in agreement with previous reports, a single 2-h exposure to immobilization stress led to a significant enhancement in anxiety-like behavior in the EPM 10 days later.

Next, a separate cohort of animals were treated with riluzole for 24 h in the drinking water, at a dosage that was previously shown to be effective in preventing the impact of stress in the rat hippocampus and PFC (31, 33, 36). Access to regular drinking water was resumed at the end of riluzole treatment (i.e. day 1, Fig. 1A). This poststress administration of riluzole increased the percentage of time spent in the open arm specifically in the stressed rats, but not in the control animals (Fig. 1B: Control + Riluzole: $55.6 \pm 3.7\%$; Stress + Riluzole: $53.1 \pm 4.0\%$, $N = 14$ rats per

group). Importantly, riluzole administration restored the stress-induced reduction in open arm time to levels that were significantly higher than those seen in the stressed animals that did not receive this poststress treatment. A similar effect was also seen 10 days later in the open arm entry in the stressed animals treated with riluzole, without any effects in the control animals (Fig. 1C: Control + Riluzole: $65.8 \pm 2.9\%$; Stress + Riluzole: $59.4 \pm 3.1\%$). As a result, the anxiety index for riluzole-treated stressed rats was comparable to the unstressed control rats that did not receive the drug (Fig. 1D: Control + Riluzole: $0.39 \pm 0.03\%$; Stress + Riluzole: $0.44 \pm 0.03\%$). Significant interaction between the factors “stress” and “riluzole” reflects corrective effects of riluzole on the delayed increase in anxiety-like behavior in stressed rats (Supplementary Table S1).

Oral administration of riluzole after acute stress prevents delayed spinogenesis in the BLA

The delayed increase in anxiety-like behavior after acute stress is accompanied by morphological changes in the principal neurons of the rat BLA (16, 30, 35). Specifically, the same acute stress exposure causes an increase in the density of spines along the primary apical dendrites of BLA neurons, also 10 days later (16). We, therefore, examined if poststress riluzole treatment also prevents the delayed BLA spinogenesis 10 days after acute stress (Fig. 2A). Hence, we prepared coronal brain sections from all four experimental groups 10 days later and labeled BLA principal neurons with Alexa Fluor-488 for quantification of dendritic spine density (Fig. 2A and B). The total number of spines along the primary apical dendrite, up to a distance of 80 μm from the origin of the dendrite, was counted (see Materials and methods). Consistent with previous reports, we found a significant increase in the total number of spines, 10 days after acute stress, compared with controls (Fig. 2C and D; Total number of spines in 80 μm , Control: 184.1 ± 8.18 , $N = 19$ rats; Stress: 238.4 ± 12.84 , $N = 15$ rats). Riluzole administered, for 24 h, after the end of 2-h stress blocked this delayed spinogenesis in the BLA (Fig. 2C and D; Control + Riluzole: 191.6 ± 10.05 , $N = 14$ rats; Stress + Riluzole: 172.3 ± 12.89 , $N = 12$ rats) (Supplementary Table S2). Next, we quantified the distribution of the spines in eight consecutive 10- μm dendritic segments along the length of the primary dendrite (adding up to a total length of 80 μm). Here too, stress led to a significant increase in the number of spines along most of the dendritic segments. Similar patterns, however, were not evident in the riluzole-treated stress group (Fig. 2E: Control: $n = 44$ dendrites, $N = 19$ rats; Stress: $n = 40$ dendrites, $N = 15$ rats; Control + Riluzole: $n = 50$ dendrites, $N = 14$ rats; Stress + Riluzole: $n = 46$ dendrites, $N = 12$ rats).

Oral administration of riluzole after acute stress prevents delayed increase in synaptic excitability in BLA neurons

Dendritic spines form the structural substrate for excitatory synaptic transmission in the rodent brain. The delayed effects of a single episode of acute stress in the BLA are manifested not only as increased spine density but also as physiological strengthening through enhanced excitatory synaptic transmission (17, 37). Since oral administration of riluzole after acute stress prevents stress-induced spinogenesis, would the same riluzole treatment also block the physiological effects at excitatory synapses?

To address this question, we used whole-cell voltage-clamp recordings in brain slices (see Materials and methods) to monitor miniature excitatory postsynaptic currents (mEPSCs) in BLA principal neurons 10 days after a single exposure to 2-h acute stress

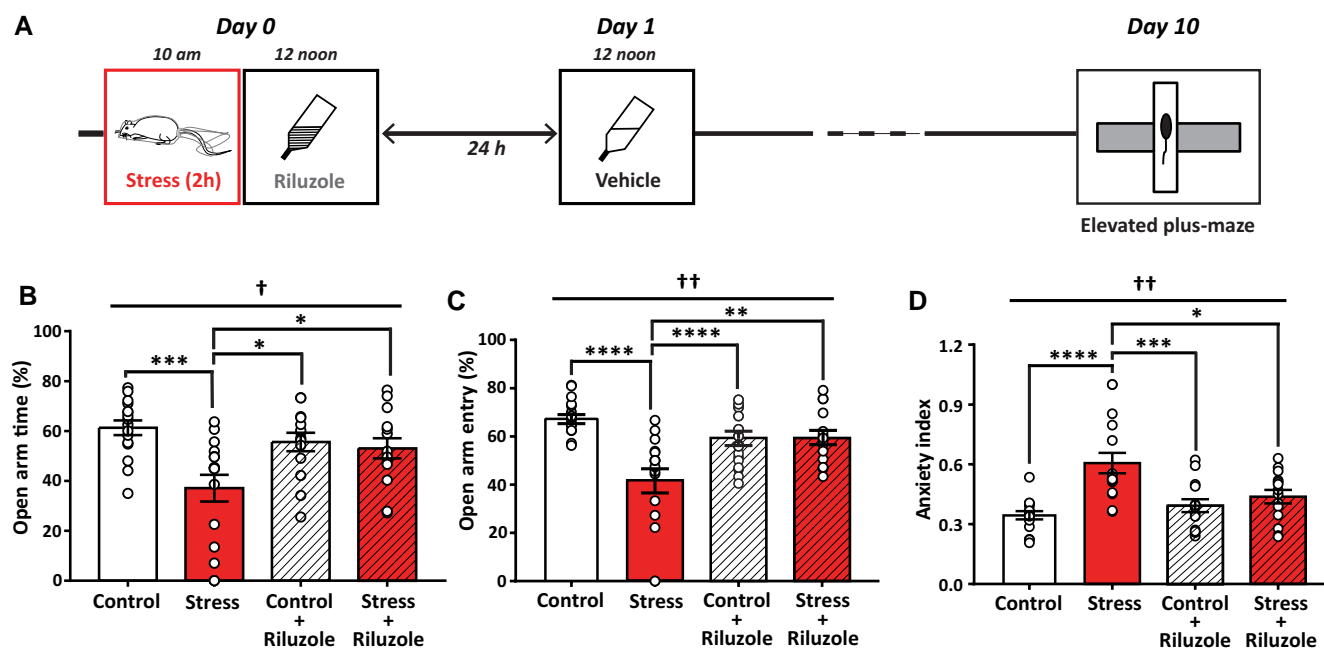


Fig. 1. Riluzole in drinking water after stress prevents the delayed increase in anxiety-like behavior. A) Experimental design depicting the timeline of single episode of immobilization stress (2 h), beginning at 10 AM on day 0. Riluzole is administered on day 0 after the end of the 2-h stress (12 PM) and continued for 24 h into day 1. On day 1 (12 PM), the drug is replaced by regular drinking water (vehicle) and continued till day 10. On day 10, anxiety-like behavior was assessed using EPM. Summary graph showing percentage of time spent in open arm B), percentage of entries into open arm C) on the elevated plus maze, and overall anxiety index D) on day 10. Two-way ANOVA, post hoc Tukey's multiple comparisons test, * $P < 0.05$, ** $P < 0.01$, *** $P < 0.001$, and **** $P < 0.0001$. † $P < 0.05$ and †† $P < 0.001$ in "interaction" between factors "stress" and "riluzole."

(Fig. 3A). As reported earlier (17, 37), stress triggered a delayed increase in the average instantaneous frequency of mEPSCs (Fig. 3B and C: Control: 1.53 ± 0.17 Hz, $n = 8$ cells, $N = 6$ rats; Stress: 2.41 ± 0.25 Hz, $n = 13$ cells, $N = 6$ rats). However, the same stress failed to elicit any increase in mEPSC frequency after oral administration of riluzole and this prevention of stress-induced enhancement of mEPSC frequency was statistically significant (Fig. 3B and C: Control + Riluzole: 1.25 ± 0.17 Hz, $n = 9$ cells, $N = 6$ rats; Stress + Riluzole: 1.49 ± 0.20 Hz, $n = 12$ cells, $N = 6$ rats) (Supplementary Table S3). The stress-induced increase in mEPSC frequency was also reflected in the cumulative frequency distribution of the interevent intervals (Fig. 3D). The distribution curve is shifted to the left in stressed animals, implying a larger number of events with lesser interevent intervals following stress, which is reflected as enhanced frequency. This shift is prevented with riluzole treatment after stress. We did not observe any effects of stress on the average amplitude of these miniature events (Fig. 3E: Control: 19.36 ± 0.99 pA; Stress: 20.18 ± 0.73 pA; Control + Riluzole: 19.62 ± 1.18 pA; Stress + Riluzole: 19.51 ± 0.69 pA).

Discussion

Here we tested if suppressing the elevation of extracellular glutamate levels, after stress exposure (13, 14, 37), prevents its delayed impact on amygdalar structure and function in rats. Specifically, we found that systemic riluzole administration, immediately after acute immobilization stress, blocked the strengthening of the morphological and physiological basis of synaptic connectivity in the BLA, as well as enhanced anxiety-like behavior, 10 days later. The findings reported here add new dimensions to previous studies on the efficacy of riluzole in countering the detrimental effects of stress. First, while earlier work focused on stress-induced changes in the hippocampus and PFC (31, 32, 40), this is the first

such report on how riluzole is effective in blocking the opposite effects of stress in the amygdala across biological scales spanning behavioral and synaptic changes (Fig. 4). Second, we explored the delayed impact of acute stress as opposed to models of chronic or repeated stress in earlier studies. For instance, riluzole administration in a rat model of repeated stress helped rescue anhedonia and helplessness behavior induced by chronic unpredictable stress (31). This same treatment also prevented stress-induced alterations in glial metabolism in the PFC (31). Notably, those earlier analyses that used chronic stress paradigms combined them with chronic riluzole treatments that overlapped with the entire duration of the chronic stress (31–33). In this context, it is interesting to note that the duration of riluzole treatment itself can give rise to strikingly different effects. For example, in a previous study (33), riluzole administration in the drinking water was initiated before stress and continued for the entire duration of 10 days of chronic immobilization stress (2 h/day). This prevented the loss of dendritic spines on hippocampal CA1 pyramidal neurons caused by chronic stress, though the drug by itself had no effect. On the other hand, the same chronic riluzole treatment in the same animals failed to prevent stress-induced spinogenesis in the BLA. However, chronic riluzole administration alone also led to spinogenesis in the BLA. Thus, the same chronic administration of riluzole that blocked the morphological effect of stress on spines in the hippocampus instead mimicked its effect on amygdalar spines (33). In contrast, here we find that a single 24-h treatment with riluzole by itself did not have any morphological or electrophysiological effects on the amygdala. We also find that the same 24-h treatment with riluzole prevents the delayed reduction in spine numbers in the CA1 region of the hippocampus (Supplementary Fig. S1). This is in agreement with the rationale of the current study that targeting the point of commonality between the two brain areas can, indeed, block the subsequent

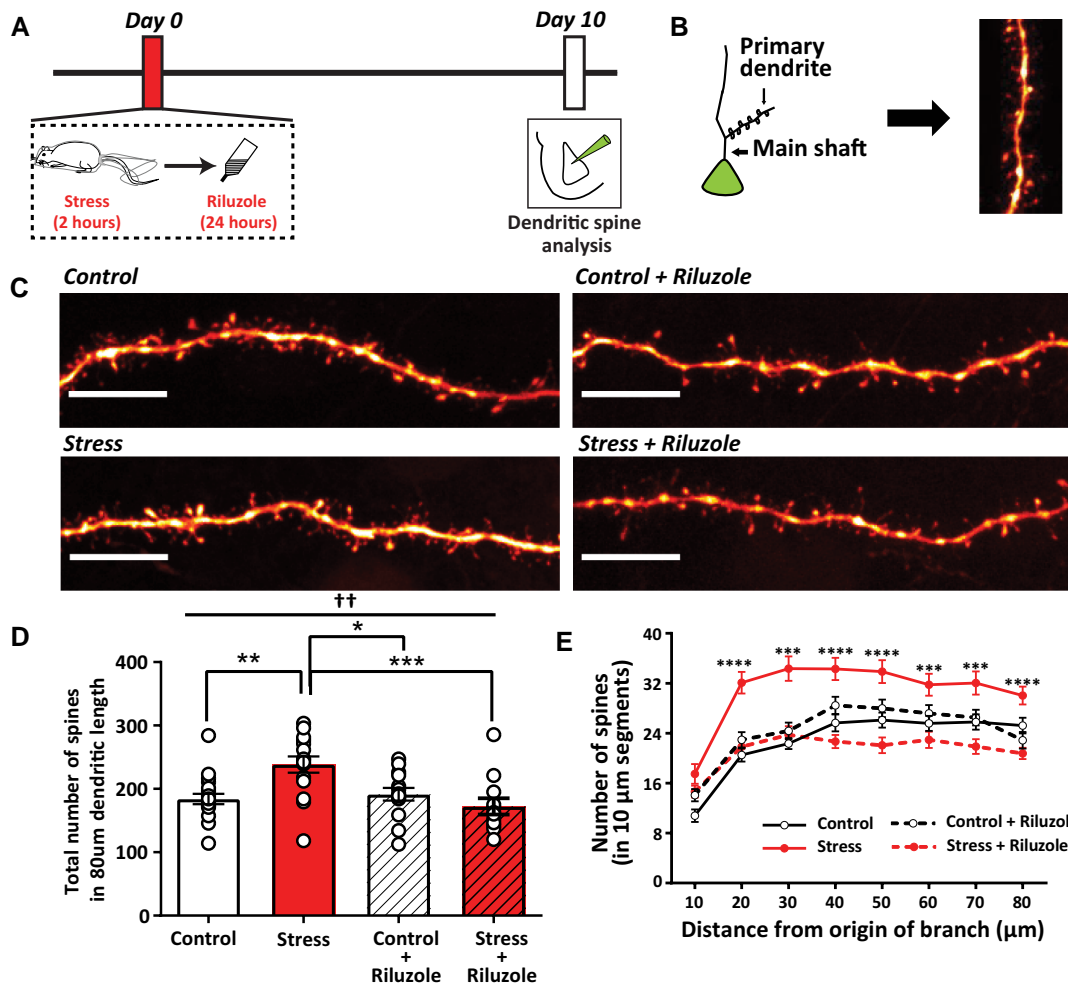


Fig. 2. Riluzole in drinking water after stress prevents the delayed increase in spine density on BLA principal neurons. A) Experimental design. Rats were subjected to a 2-h stress followed by 24-h riluzole treatment on day 0. Iontophoretic dye labeling carried out on individual BLA principal neurons on day 10. B) Spines were quantified only on the primary dendrites emanating from the main shaft of the principal neuron. C) Representative confocal images of dendritic segments and spines from BLA neurons in vehicle- and riluzole-treated animals (scale = 10 μm). D) Summary bar graph showing total number of spines in 80 μm length of primary dendrite. Ordinary two-way ANOVA, post hoc Tukey's multiple comparisons test, * $P < 0.05$, ** $P < 0.01$, *** $P < 0.001$, and $\dagger\dagger P < 0.01$ in "interaction" between factors stress and riluzole. E) Plot showing number of spines in successive 10- μm segments along the length of a primary dendrite. Repeated measures two-way ANOVA, post hoc Tukey's multiple comparisons test for "stress" versus "stress + riluzole." *** $P < 0.001$ and **** $P < 0.0001$.

expression of opposite forms of spine plasticity. Third, unlike these earlier studies, riluzole was administered after the end of acute stress. While this was effective in blocking the delayed effects 10 days later, it remains to be seen if riluzole administration is necessary immediately after the stress has occurred or whether it will also be effective when used at later time points after acute stress, and how long this poststress window of opportunity extends. Finally, the administration of riluzole through drinking water offers an advantage over other methods like oral gavage or intraperitoneal injections, which have been shown to enhance corticosterone and interfere with the effects of stress (29, 30, 35, 38, 39). This experimental paradigm of oral administration of riluzole after stress also bears greater similarity to a clinically realistic framework.

Riluzole is known to reduce glutamatergic transmission through its action on several targets. Apart from enhancing glial uptake of glutamate (19, 20) and reducing presynaptic glutamate release (22), it has also been reported to act as an antagonist of NMDA and AMPA subtypes of glutamate receptors (18, 23). However, the precise mechanisms by which riluzole blocks the

delayed effects of stress requires further analyses. It is interesting to note that the astrocytic glutamate transporter, GLT-1, which plays a major role in glutamate uptake in the CNS, is potentiated by riluzole (20). Riluzole has a higher affinity for these glial glutamate uptake transporters than for other targets (19) enabling their activation at lower concentrations of this drug. Notably, the concentration of riluzole used in our study is comparable to the EC_{50} of riluzole's effects on GLT-1. A similar dosage of riluzole was used in previous studies involving the hippocampus and the PFC (31, 33, 36), thereby providing a basis for comparing the findings reported here in the BLA. Future studies will be needed to examine how amygdalar glial cells themselves are affected by the same riluzole treatment, which may provide direct evidence into their contribution to prevention of stress-induced neuronal plasticity.

Interestingly, in addition to ALS, riluzole has also been used for treating PTSD, depression, and other psychiatric disorders (21, 28, 41–49). However, these share a common feature in that the drug was administered after patients were found to be resistant to other therapeutic interventions. Thus, the affected individuals, in addition to suffering from long-standing psychiatric disorders,

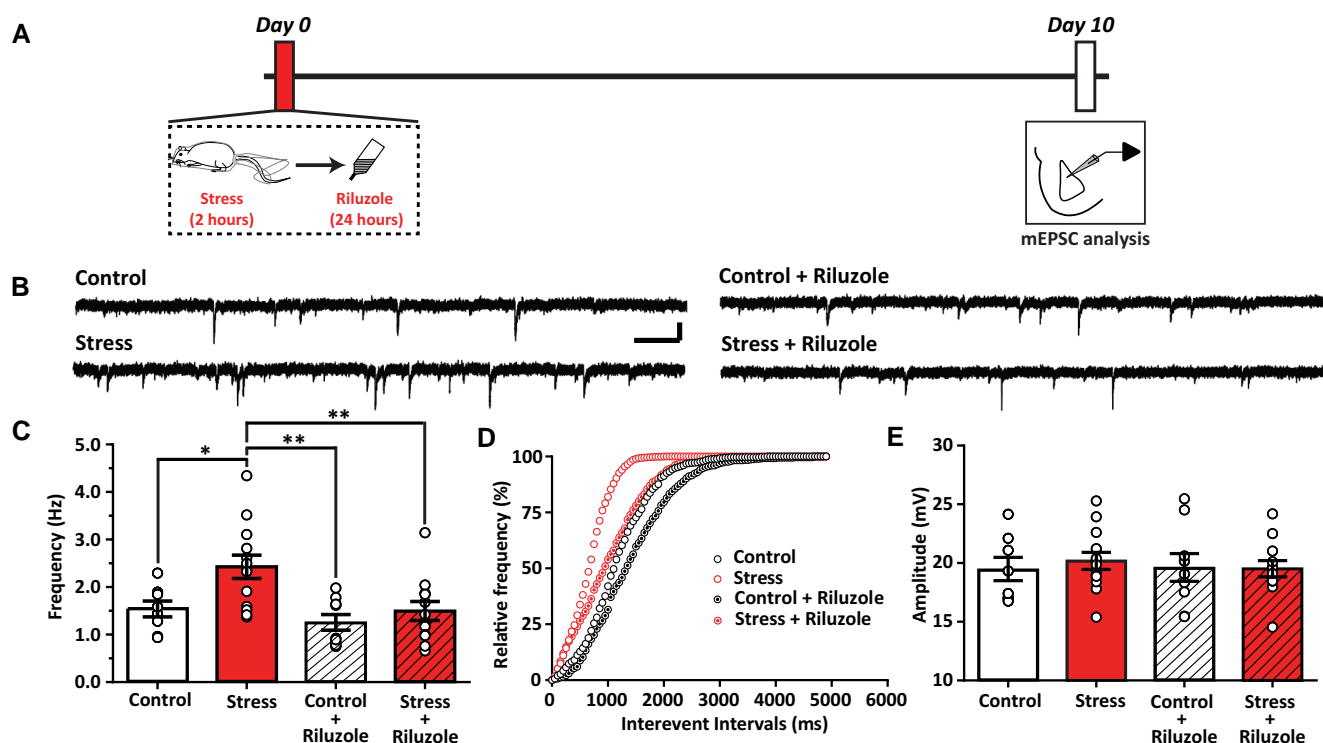


Fig. 3. Poststress riluzole administration in drinking water prevents the delayed increase in frequency of mEPSCs on BLA principal neurons. A) Experimental design. Rats were subjected to a 2-h stress followed by 24-h riluzole treatment on day 0. Whole-cell patch clamp recordings of mEPSCs were carried out on BLA principal neurons on day 10. B) Representative traces of mEPSCs from BLA principal neurons in vehicle- and riluzole-treated animals (scale: 20 pA, 0.5 s). C) Summary graph showing frequency of mEPSCs on day 10. Two-way ANOVA, post hoc Sidak's multiple comparisons test, * $P < 0.05$ and ** $P < 0.01$. D) Cumulative frequency distribution of mEPSCs in vehicle- and riluzole-treated groups. E) Graph showing average amplitude of mEPSCs in all groups.

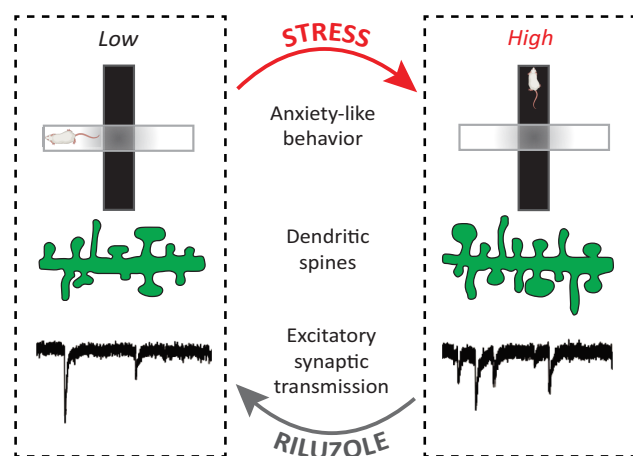


Fig. 4. Summary. Acute stress (top) causes a delayed increase in anxiety-like behavior, BLA spine density, and mEPSC frequency. These behavioral and synaptic changes are blocked by poststress riluzole treatment (bottom).

were also subjected to other pharmacological treatments before riluzole was administered. Commonly used animal models of stress, however, do not capture these complexities. For example, we have previously reported (33) how chronic riluzole administration, initiated before stress, mimics the effects of stress in the BLA. In contrast, the present study shows that a single 24-h riluzole treatment has no effect by itself. Notably, here riluzole was administered immediately after the stressful experience, without the time delays, between the triggering event and therapeutic

intervention, that are common in clinical settings. This highlights the timing of therapeutic interventions as an important factor in developing optimal strategies to counter the debilitating effects of stress disorders.

Materials and methods

Animals and stress protocol

All experiments were performed on male Wistar rats (postnatal 55–60 days of age) maintained on a 14 h:10 h light–dark cycle, with ad libitum food and water. All procedures related to animal care and usage were approved by Institutional Ethics Committee at the National Centre for Biological Sciences, India. Rats were subjected to a single episode of immobilization stress on day 0 (Fig. 1), between 10 AM and 12 PM, without any access to food and water. At the end of the stress episode, the rats were returned to their home cages and remained unperturbed until day 10. All experiments were performed on day 10. The control rats were not subjected to any such stress episodes and were housed in separate rooms.

Drug administration

Riluzole (Sigma, St. Louis, MO) was administered to the rats for 24 h in their drinking water (4 mg/kg body weight/day), as established previously (31, 33, 36). Rats subjected to immobilization stress had access to riluzole in their home cage soon after the termination of the immobilization episode on day 0 (Fig. 1). The control rats from the same cohort also received riluzole for 24 h on the same day. This was replaced by regular drinking water following

the 24-h riluzole treatment. Riluzole solution (~30 µg/mL, based on average water consumption/cage/day) was prepared by dissolving the drug in drinking water by constant stirring overnight ~6–10 h in a light-protected container.

EPM

Rats were subjected to EPM test 10 days after the exposure to single episode of immobilization stress (30). Control rats from the same cohort were subjected to EPM on the same day. Following ~20 min of habituation in a holding room, rats were placed in the center of the EPM with a free choice to explore open arms (~75 lx) and closed arms (~0 lx) for 5 min. All trials were video recorded and analyzed offline by the experimenter blind to the assigned group of the animals. The time spent in open arms, number of open arm entries, and anxiety index was calculated as described (30), using the following equation:

$$\text{Anxiety Index} = 1 - [(\text{Open Arm Time} / \text{Total Time} + \text{Open Arm Entries} / \text{Total Entries}) / 2].$$

Intracellular dye fills

Ten days after acute immobilization stress exposure, the stressed and age-matched control animals (~postnatal day 70) were anesthetized with an overdose of ketamine and xylazine (3:1, 0.9 mL ketamine; 0.3 mL xylazine) and perfused transcardially with 50 mL of 0.1 M phosphate buffer (PB) followed by 100 mL of fixative solution containing 4% 0.1 M sodium phosphate-buffered paraformaldehyde (pH 7.4) (at 4°C). Subsequently, the brains were gently removed from the skull and post fixation was done for 3 h in the abovementioned fixative (ice cold) on a rocker (at 4°C). Coronal sections of the brain containing the amygdala and dorsal hippocampus were obtained using VT1200S vibratome (Leica Biosystems, Germany) and stored in 0.1 M PB for intracellular fills (section thickness: 100 µm).

Neurons were dye labeled using methodology described previously (50). Briefly, the sections were placed in cold PB and the region of interest was identified with an infrared differential interference contrast (DIC)/epifluorescent microscope (SliceScope, Scientifica, UK) using a 4x air objective (Olympus, Japan). The large soma of principal neurons (diameter ~15 µm) was identified within the BLA using a 40x water immersion objective (Olympus, Japan). The cell bodies were then impaled with sharp glass micropipette containing 10 mM Alexa Fluor-488 hydrazide, sodium salt solution (Thermo Fisher Scientific, CA, USA). Iontophoretic dye injection into the cells was performed by applying a 0.5-s negative current pulse (1 Hz) using Master8 (A.M.P.I. Systems, Israel) until the distal dendrites were sufficiently filled (~15 min). The sections were then placed in cold 4% paraformaldehyde-PB for 30 min followed by DAPI (Sigma, St. Louis, MO) staining for 15 min. The sections were then mounted in ProlongGold antifade reagent (Thermo Fisher Scientific, CA, USA).

Image visualization and analysis

Image acquisition was done using confocal laser scanning microscopy on Olympus Fluoview3000 (Olympus, Japan). Primary dendritic segments of dye-filled neurons were visualized under a 60x oil objective and confocal stacks were acquired at a Z-step size of 0.35 µm (Nyquist sampling criteria) capturing the dendrite origin point and a dendrite length of ~100 µm. The confocal stacks of individual primary dendrites were used to quantify the number

of spines using filaments plug-in on IMARIS (Oxford instruments, Bitplane, Switzerland).

Electrophysiology

Rats were deeply anaesthetized with halothane, decapitated, and the brain removed rapidly. The brain was dissected in ice-cold artificial cerebrospinal fluid (aCSF) containing (in mM): NaCl, 86; glucose, 25; sucrose, 75; NaHCO₃, 25; NaH₂PO₄, 1.2; KCl, 2.5; CaCl₂, 0.5; and MgCl₂, 7 (pH 7.4, 320 mOsm), and 400-µm coronal sections were cut using VT1200S vibratome (Leica Biosystems, Germany). The sections were allowed to recover for at least 30 min in recording aCSF (in mM): NaCl, 124; glucose, 20; NaHCO₃, 25; NaH₂PO₄, 1.2; KCl, 2.5; CaCl₂, 2; and MgCl₂, 1 (pH 7.4, 320 mOsm), which was equilibrated with 95% O₂/5% CO₂ before being transferred to a submerged chamber for whole-cell recordings from BLA principal neurons under IR-DIC visualization (BX51WI, Olympus).

mEPSCs were recorded from principal neurons in the BLA using whole-cell pipettes (3–5 MΩ) filled with (in mM): CsOH, 110; D-gluconic acid, 110; CsCl, 20; HEPES, 10; NaCl, 4; QX-314, 5; phosphocreatine, 10; Mg-ATP, 4; Na₂-GTP, 0.3; and EGTA 0.2 (pH 7.3–7.4, 280–285 mOsm). Recordings were obtained using a HEKA EPC10 Plus amplifier (Heka Elektronik) filtered at 2.9 kHz and digitized at 10 kHz. Only cells with membrane potentials less than –60 mV were included. Recordings were discarded if series resistance (Rs) changed by more than 20% from beginning to end or if Rs exceeded 25 MΩ. Cells were held at –70 mV and mEPSCs were pharmacologically isolated by adding TTX (0.5 µM) and picrotoxin (100 µM) to the recording aCSF. Continuous current traces of 5-min duration were analyzed using MiniAnalysis (Synaptosoft, NJ).

Statistical analysis

All statistical analyses were performed in GraphPad Prism (GraphPad software Inc., La Jolla, CA, USA.). Results are expressed as mean ± SEM. Specific details of tests are mentioned in figure legends. Assumptions of equal variance across groups and random sampling from normally distributed data were considered for all ANOVA analyses.

Acknowledgments

We are deeply grateful to Dr. Siddhartha Datta for his immense contribution towards this project before his untimely demise in 2021. We also thank the Central Imaging and Flow Cytometry Facility, Bangalore Life Science Cluster, for providing us with imaging resources. We are also thankful to Biorender.com for helping us with illustrations for this manuscript.

Supplementary material

[Supplementary material](#) is available at PNAS Nexus online.

Funding

This work was supported by intramural funds from NCBS-TIFR, Department of Atomic Energy, Government of India (S.D., Z.R., S.N., and S.C.). S.D. was also supported by the SERB-National Post Doctoral Fellowship, Government of India.

Author contributions

S.D., Z.R., S.N., and S.C. designed the study. S.D. and Z.R. collected the data. S.D., Z.R., and S.N. compiled and analyzed the data. Z.R., S.N., and S.C. wrote the manuscript. S.C. supervised the study, provided funding and resources for the study, and edited the manuscript.

Data availability

All data are included in the manuscript.

References

- Ressler KJ. 2010. Amygdala activity, fear, and anxiety: modulation by stress. *Biol Psychiatry*. 67(12):1117–1119.
- Zhang WH, Zhang JY, Holmes A, Pan BX. 2021. Amygdala circuit substrates for stress adaptation and adversity. *Biol Psychiatry*. 89(9):847–856.
- Chattarji S, Tomar A, Suvrathan A, Ghosh S, Mostafizur Rahman M. 2015. Neighborhood matters: divergent patterns of stress-induced plasticity across the brain. *Nat Neurosci*. 18(10):1364–1375.
- McEwen BS, Nasca C, Gray JD. 2016. Stress effects on neuronal structure: hippocampus, amygdala, and prefrontal Cortex. *Neuropsychopharmacol*. 41(1):3–23.
- Aubry AV, Serrano PA, Burghardt NS. 2016. Molecular mechanisms of stress-induced increases in fear memory consolidation within the amygdala. *Front Behav Neurosci*. 10:191.
- Shors TJ, Weiss C, Thompson RF. 1992. Stress-induced facilitation of classical conditioning. *Science* 257(5069):537–539.
- Suvrathan A, et al. 2014. Stress enhances fear by forming new synapses with greater capacity for long-term potentiation in the amygdala. *Philos Trans R Soc Lond B: Biol Sci*. 369(1633):20130151.
- Vyas A, Chattarji S. 2004. Modulation of different states of anxiety-like behavior by chronic stress. *Behav Neurosci*. 118(6):1450–1454.
- Geuze E, Vermetten E, Ruf M, de Kloet CS, Westenberg HGM. 2008. Neural correlates of associative learning and memory in veterans with posttraumatic stress disorder. *J Psychiatric Res*. 42(8):659–669.
- Rauch SL, et al. 2000. Exaggerated amygdala response to masked facial stimuli in posttraumatic stress disorder: a functional MRI study. *Biol Psychiatry*. 47(9):769–776.
- Sheline YI, et al. 2001. Increased amygdala response to masked emotional faces in depressed subjects resolves with antidepressant treatment: an fMRI study. *Biol Psychiatry*. 50(9):651–658.
- Woon FL, Hedges DW. 2009. Amygdala volume in adults with posttraumatic stress disorder: a meta-analysis. *J Neuropsychiatry Clin Neurosci*. 21(1):5–12.
- Popoli M, Yan Z, McEwen BS, Sanacora G. 2012. The stressed synapse: the impact of stress and glucocorticoids on glutamate transmission. *Nat Rev Neurosci*. 13(1):22–37.
- Reznikov LR, et al. 2007. Acute stress-mediated increases in extracellular glutamate levels in the rat amygdala: differential effects of antidepressant treatment. *Eur J Neurosci*. 25(10):3109–3114.
- Lakshminarasimhan H, Chattarji S. 2012. Stress leads to contrasting effects on the levels of brain derived neurotrophic factor in the hippocampus and amygdala. *PLoS One* 7(1):e30481.
- Mitra R, Jadhav S, McEwen BS, Vyas A, Chattarji S. 2005. Stress duration modulates the spatiotemporal patterns of spine formation in the basolateral amygdala. *Proc Natl Acad Sci U S A*. 102(26):9371–9376.
- Yasmin F, Saxena K, McEwen BS, Chattarji S. 2016. The delayed strengthening of synaptic connectivity in the amygdala depends on NMDA receptor activation during acute stress. *Physiol Rep*. 4(20):e13002.
- Debono MW, le Guern J, Canton T, Doble A, Pradier L. 1993. Inhibition by riluzole of electrophysiological responses mediated by rat kainate and NMDA receptors expressed in *Xenopus* oocytes. *Eur J Pharmacol*. 235(2–3):283–289.
- dos Santos Frizzo ME, Dall'Onder LP, Dalcin KB, Souza DO. 2004. Riluzole enhances glutamate uptake in rat astrocyte cultures. *Cell Mol Neurobiol*. 24(1):123–128.
- Fumagalli E, Funicello M, Rauen T, Gobbi M, Mennini T. 2008. Riluzole enhances the activity of glutamate transporters GLAST, GLT1 and EAAC1. *Eur J Pharmacol*. 578(2–3):171–176.
- Pittenger C, et al. 2008. Riluzole in the treatment of mood and anxiety disorders. *CNS Drugs* 22(9):761–786.
- Prakriya M, Mennerick S. 2000. Selective depression of low-release probability excitatory synapses by sodium channel blockers. *Neuron* 26(3):671–682.
- Zona C, et al. 2002. Kainate-induced currents in rat cortical neurons in culture are modulated by riluzole. *Synapse* 43(4):244–251.
- Bensimon G, Lacomblez L, Meininger V. 1994. A controlled trial of riluzole in amyotrophic lateral sclerosis. ALS/Riluzole Study Group. *N Engl J Med*. 330(9):585–591.
- Berry JD, et al. 2013. The Combined Assessment of Function and Survival (CAFS): a new endpoint for ALS clinical trials. *Amyotroph Lateral Scler Frontotemporal Degener*. 14(3):162–168.
- Fang T, et al. 2018. Stage at which riluzole treatment prolongs survival in patients with amyotrophic lateral sclerosis: a retrospective analysis of data from a dose-ranging study. *Lancet Neurol*. 17(5):416–422.
- Lacomblez L, Bensimon G, Leigh PN, Guillet P, Meininger V. 1996. Dose-ranging study of riluzole in amyotrophic lateral sclerosis. *Lancet* 347(9013):1425–1431.
- Frizzo ME. 2019. The effect of glutamatergic modulators on extracellular glutamate: how does this information contribute to the discovery of novel antidepressants? *Curr Ther Res Clin Exp*. 91:25–32.
- Chakraborty P, Chattarji S. 2019. Interventions after acute stress prevent its delayed effects on the amygdala. *Neurobiol Stress*. 10:100168.
- Chakraborty P, Datta S, McEwen BS, Chattarji S. 2020. Corticosterone after acute stress prevents the delayed effects on the amygdala. *Neuropsychopharmacol*. 45(13):2139–2146.
- Banasr M, et al. 2010. Glial pathology in an animal model of depression: reversal of stress-induced cellular, metabolic and behavioral deficits by the glutamate-modulating drug riluzole. *Mol Psychiatry*. 15(5):501–511.
- Gourley SL, Espitia JW, Sanacora G, Taylor JR. 2012. Antidepressant-like properties of oral riluzole and utility of incentive disengagement models of depression in mice. *Psychopharmacology (Berl)*. 219(3):805–814.
- Naskar S, Datta S, Chattarji S. 2022. Riluzole prevents stress-induced spine plasticity in the hippocampus but mimics it in the amygdala. *Neurobiol Stress*. 18:100442.
- Sugiyama A, et al. 2012. Riluzole produces distinct anxiolytic-like effects in rats without the adverse effects associated with benzodiazepines. *Neuropharmacology* 62(8):2489–2498.
- Rao RP, Anilkumar S, McEwen BS, Chattarji S. 2012. Glucocorticoids protect against the delayed behavioral and

- cellular effects of acute stress on the amygdala. *Biol Psychiatry*. 72(6):466–475.
- 36 Pereira AC, et al. 2014. Glutamatergic regulation prevents hippocampal-dependent age-related cognitive decline through dendritic spine clustering. *Proc Natl Acad Sci U S A*. 111:18733–8.
- 37 Yasmin F, et al. 2020. Stress-induced modulation of endocannabinoid signaling leads to delayed strengthening of synaptic connectivity in the amygdala. *Proc Natl Acad Sci U S A*. 117(1):650–655.
- 38 Cohen H, Matar MA, Buskila D, Kaplan Z, Zohar J. 2008. Early post-stressor intervention with high-dose corticosterone attenuates posttraumatic stress response in an animal model of post-traumatic stress disorder. *Biol Psychiatry*. 64(8):708–717.
- 39 Zohar J, et al. 2011. High dose hydrocortisone immediately after trauma may alter the trajectory of PTSD: interplay between clinical and animal studies. *Eur Neuropsychopharmacol*. 21(11):796–809.
- 40 Fullana MN, et al. 2019. Regionally selective knockdown of astroglial glutamate transporters in infralimbic cortex induces a depressive phenotype in mice. *Glia* 67(6):1122–1137.
- 41 de Boer JN, et al. 2019. Efficacy and tolerability of riluzole in psychiatric disorders: a systematic review and preliminary meta-analysis. *Psychiatry Res*. 278:294–302.
- 42 Zarate CA, Manji HK. 2008. Riluzole in psychiatry: a systematic review of the literature. *Expert Opin Drug Metab Toxicol*. 4(9):1223–1234.
- 43 Brennan BP, et al. 2010. Rapid enhancement of glutamatergic neurotransmission in bipolar depression following treatment with riluzole. *Neuropsychopharmacol*. 35(3):834–846.
- 44 Salardini E, et al. 2016. Riluzole combination therapy for moderate-to-severe major depressive disorder: a randomized, double-blind, placebo-controlled trial. *J Psychiatr Res*. 75:24–30.
- 45 Sanacora G, et al. 2007. Preliminary evidence of riluzole efficacy in antidepressant-treated patients with residual depressive symptoms. *Biol Psychiatry*. 61(6):822–825.
- 46 Spangler PT, et al. 2020. Randomized controlled trial of riluzole augmentation for posttraumatic stress disorder: efficacy of a glutamatergic modulator for antidepressant-resistant symptoms. *J Clin Psychiatry*. 81(6):18364.
- 47 Bernard R, et al. 2011. Altered expression of glutamate signaling, growth factor, and glia genes in the locus coeruleus of patients with major depression. *Mol Psychiatry*. 16(6):634–646.
- 48 Choudary PV, et al. 2005. Altered cortical glutamatergic and GABAergic signal transmission with glial involvement in depression. *Proc Natl Acad Sci U S A*. 102(43):15653–15658.
- 49 Miguel-Hidalgo JJ, et al. 2010. Glial and glutamatergic markers in depression, alcoholism, and their comorbidity. *J Affect Disord*. 127(3):230–240.
- 50 Naskar S, Chattarji S. 2019. Stress elicits contrasting effects on the structure and number of astrocytes in the amygdala versus hippocampus. *eNeuro* 6(1):ENEURO.0338–18.2019.